Molecular Engineering of an Alkaline Naphthoquinone Flow Battery

Molecular Engineering of an Alkaline Naphthoquinone Flow Battery

Liuchuan Tong, Marc-Antoni Goulet, Daniel P. Tabor, Emily F. Kerr, Diana De Porcellinis, Eric M. Fell, Alán Aspuru-Guzik, Roy G. Gordon, and Michael J. Aziz**

Dr. Liuchuan Tong, Dr. Daniel P. Tabor, Dr. Alán Aspuru-Guzik, Dr. Roy G. Gordon
Department of Chemistry and Chemical Biology, Harvard University, 12 Oxford Street, Cambridge, Massachusetts 02138, USA

Dr. Marc-Antoni Goulet, Dr. Diana De Porcellinis, Eric M. Fell, Dr. Michael J. Aziz
Harvard John A. Paulson School of Engineering and Applied Sciences, 29 Oxford Street, Cambridge, Massachusetts 02138, USA

Present Addresses
Dr. Marc-Antoni Goulet
Form Energy Inc., Somerville, Massachusetts 02143, United States
Dr. Alán Aspuru-Guzik
Department of Chemistry and Department of Computer Science; Vector Institute for Artificial Intelligence, University of Toronto, Toronto, Ontario, M5S 1A1, Canada

*Corresponding authors:

Roy G. Gordon
Cabot Professor
Dept. of Chemistry and Chemical Biology
Harvard University
12 Oxford Street, MA 02138, USA
Tel: +1 617-495-4017
Fax: +1 617-495-4723
email: Gordon@chemistry.Harvard.edu

Michael J. Aziz
Gene and Tracy Sykes Professor of Materials and Energy Technologies
Harvard John A. Paulson School of Engineering and Applied Sciences, Pierce Hall 204a
29 Oxford Street, MA 02138, USA
Tel: +1 (617) 495-9884
email: maziz@harvard.edu

Keywords: energy storage, flow battery, naphthoquinone, degradation mechanism

Abstract: Aqueous organic redox flow batteries (AORFBs) have recently gained significant attention as a potential candidate for grid-scale electrical energy storage. Successful implementation of this technology will require redox-active organic molecules with many desired properties. Here we introduce a naphthoquinone dimer, bislawsone, as the redox-active material in a negative potential electrolyte (negolyte) for an AORFB. This novel dimerization strategy substantially improves the performance of the electrolyte vs. that of the lawsone monomer in terms of solubility, stability, reversible capacity, permeability and cell voltage. An AORFB pairing bislawsone with a ferri/ferrocyanide positive electrolyte delivers an open-circuit voltage of 1.05 V and cycles at a current density of 300 mA/cm^2 with a negolyte concentration of 2 M electrons in alkaline solution. We determined the degradation mechanism for the naphthoquinone-based electrolyte using chemical analysis, and predict theoretically electrolytes based on naphthoquinones that will be even more stable.

1. Introduction

The cost of renewable solar and wind electricity has dropped so much that the greatest barrier to their widespread adoption is their intrinsic intermittency. A cost-effective, long discharge duration electrical energy storage solution could solve the problem of unbalanced supply and demand. Among the various proposed technologies, redox-flow batteries[1] are particularly attractive for long discharge duration because liquid redox-active electrolytes can be stored in external tanks that are separated from the power generating stack. With this design, energy capacity can be scaled independently of power capacity by simply changing the volume of electrolyte.

Recent years have seen a great deal of research into developing organic redox-active species for aqueous flow battery electrolytes. These redox-active materials are based on earth-abundant elements such as carbon, nitrogen, oxygen and sulfur, and usually utilize well-known redox-active compounds such as quinones,[2-9] viologens,[10-13] ferrocenes,[14-15] aza-

aromatics,[16-18] and nitroxide radicals[10-11, 19]. Organic-based aqueous flow batteries offer several advantages over vanadium and non-aqueous based flow batteries in cost, scalability and safety. In addition, the use of organic molecules in flow batteries opens a vast chemical space for tailoring the properties of redox-active electrolytes, including solubility, reduction potential, rate capacity, and stability. Within the quinone family, benzoquinones[6] and anthraquinones[2, 4, 7, 9] have been explored extensively as redox-active electrolytes in aqueous organic flow batteries. To date, however, there are limited reports on using naphthoquinone as an active electrolyte due not only to stability and solubility concerns but also because naphthoquinone reduction potentials tend to be intermediate between those of benzoquinones and anthraquinones, making them unsuitable for either terminal of an aqueous flow battery. 2-hydroxynaphthoquinone, commonly known as lawsone, is a natural product extracted from the leaves of the henna plant and the flower of the water hyacinth, which makes its use or derivatives of it particularly appealing from a cost and scalability perspective.[20] Lawsone has been explored as a candidate for alkaline flow batteries;[21-22] however, poor cycling stability has limited further investigation into this class of molecules. It is hypothesized that the C-H position next to the quinone functional group in the molecule is prone to Michael addition, particularly in alkaline media, and subsequent degradation from hydroxide or other nucleophiles during cycling[6, 23-24]. Efforts to modify the molecule have been made by installing a carboxyl group onto the open aromatic C-H position. Despite the increased solubility of this derivative, capacity utilization, cycling stability, and permeability remain as issues. [25]

Here, we report a naphthoquinone dimer 2,2'-bis(3-hydroxy-1,4-naphthoquinone), or bislawsone, as a high capacity, reversible negolyte material for aqueous organic flow batteries. Bislawsone was constructed by taking advantage of the reactive open site and linking two lawsone units via their 3-position. We demonstrate that this dimerization strategy improves solubility, stability, reduction potential, and permeability without compromising the capacity

per molecular weight. We also elucidate the degradation mechanism of bislawsone and propose strategies to further stabilize the molecule based on theoretical calculations. We draw important implications for the synthetic strategy and rational design of stable quinone molecules for AORFBs.

2. Results and Discussion

Synthesis and physical properties study. Bislawsone was synthesized via a one-step radical dimerization of the natural product lawsone using inexpensive chemicals and solvents (**Figure 1A**, Figure S1, S2). No further steps were necessary to purify this yellow powder. Its physical and electrochemical properties were evaluated. Cyclic voltammetry of bislawsone in 1M KOH showed a reduction potential of -0.551 V vs. standard hydrogen electrode (SHE) with a peak separation (ΔE) of 71 mV for 4 electrons. The reduction potential is 50 mV more negative than that of the lawsone monomer with overlapping peaks for the two subunits (Figure S3A), indicating higher cell voltage, and improved reversibility despite the doubling of the molecular size and the number of electrons transferred. Pairing this electrolyte with potassium ferrocyanide should yield an equilibrium cell potential of 1.05 V (**Figure 1B**). Based on the sharpness of the CV peaks, the two redox centers in the molecule do not appear to interact with each other; this conclusion is also supported by theoretical calculations (Figure 4). The pKa values (~ 6.5) for each of the hydroxyl groups in the molecule are indistinguishable by titration and are slightly higher than that of lawsone (**Figure 1C**, Figure S3B, Table S1). The two low pKa phenols in bislawsone serve as the solubilizing groups in alkaline solution. To our surprise, the solubility of bislawsone reached 0.56 M (2.24 M electrons or 60.0 Ah/L) in pH 14 solution, as compared to the 0.48 M (0.96 M electrons) solubility of lawsone in pH 14 solution. The origin of this increased solubility is hypothesized to be from the non-planar nature of the dimer along the 3,3`-single bond. The non-planar

feature may disrupt crystal packing, which would raise the solubility of the whole molecule compared to that of the planar monomer. The increased solubility of the dimer is in contrasted with the usually decreased solubility of many extended polymers compared to their parent monomers.[26]

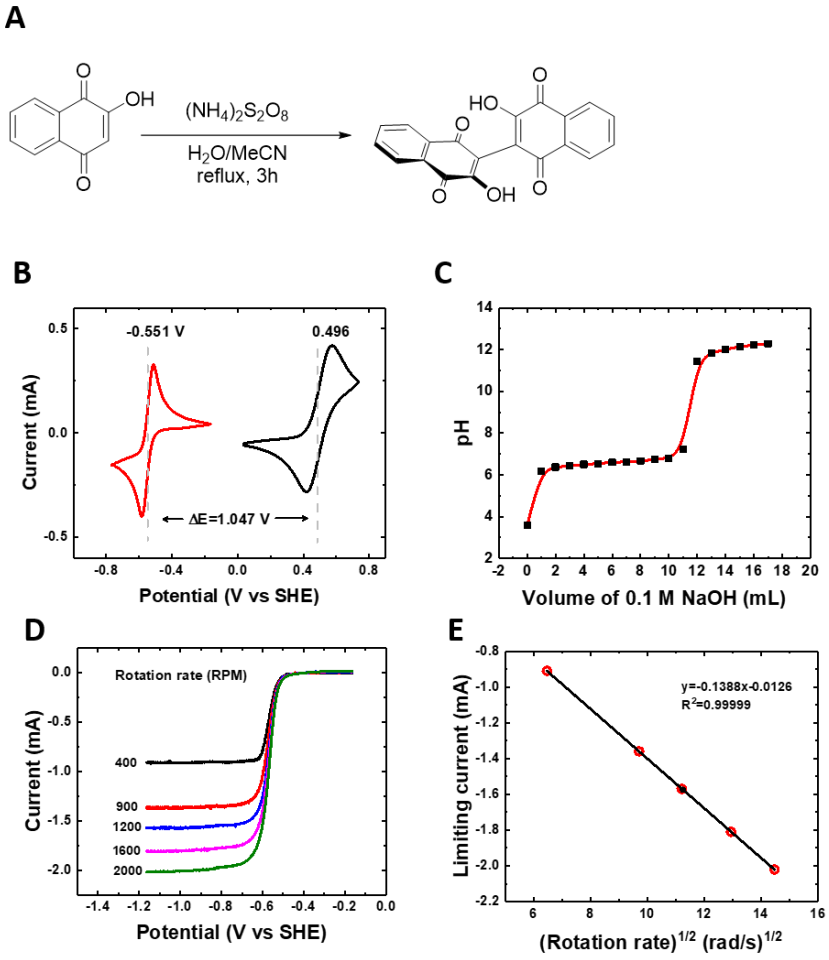

Figure 1. Synthesis and physical Characterization of bislawsone. (A) Synthetic scheme of bislawsone. (B) Cyclic voltammograms of 5 mM bislawsone (red), and 10 mM potassium ferrocyanide (black) in 1M KOH at a scan rate of 50 mV/s. The redox potential vs SHE is indicated. (C) Titration of 10 mL 0.05 M bislawsone using 0.1M NaOH solution. (D) Rotating disk electrode (RDE) measurements of bislawsone using a glassy carbon electrode in 1 M KOH at 5 rotation rates. (E) Levich plot of limiting current versus square root of rotation rate ($\omega^{1/2}$)

A dimerization strategy, as employed in the case of bislawsone, should offer the advantage of lowered permeability without significantly compromising the diffusivity or viscosity. The diffusion coefficient (*D*) of bislawsone was determined by rotating disk

electrode measurement and calculated according to the Levich plot of limiting current versus square root of rotation rate to be 4.54×10^{-6} cm^2/s (**Figure 1D, 1E**), which is in line with those of most small organic molecules. [2, 4, 6, 9, 25] The viscosity of bislawsone dissolved in 1M KOH was consistently below 2 cP for concentrations up to the solubility limit (Figure S4), which bodes well for minimizing energy inefficiency due to pumping loss. The crossover rates of bislawsone and lawsone through a Fumasep E-620K cation exchange membrane were measured in a two-compartment rotating cell (Figure S5). The permeability of bislawsone was determined to be 1.19×10^{-11} cm^2/s, which is an order of magnitude lower than the value of 1.01×10^{-10} cm^2/s for lawsone, as expected.

Synthesis and physical properties study. We assembled an alkaline flow battery with a positive electrolyte (posolyte) comprising 44 mL 0.2 M potassium ferrocyanide and 0.02 M potassium ferricyanide and a negative electrolyte (negolyte) comprising 8 mL 0.1 M (0.4 M electrons) bislawsone in 1M KOH solution (see “Full Cell Measurement” in the supporting information), separated by a Fumasep E620K cation-exchange membrane. This non-fluorinated membrane has been shown to provide very low permeability to ferro/ferricyanide and to anthraquinones.[9] These solutions were pumped through a flow cell constructed from graphite flow plates and carbon paper electrodes. During charging, the negolyte biquinone was reduced into bihydroquinone while the ferrocyanide was oxidized into ferricyanide. An excess amount of ferrocyanide was used in the cell testing in order to isolate the negolyte as the capacity limiting side.

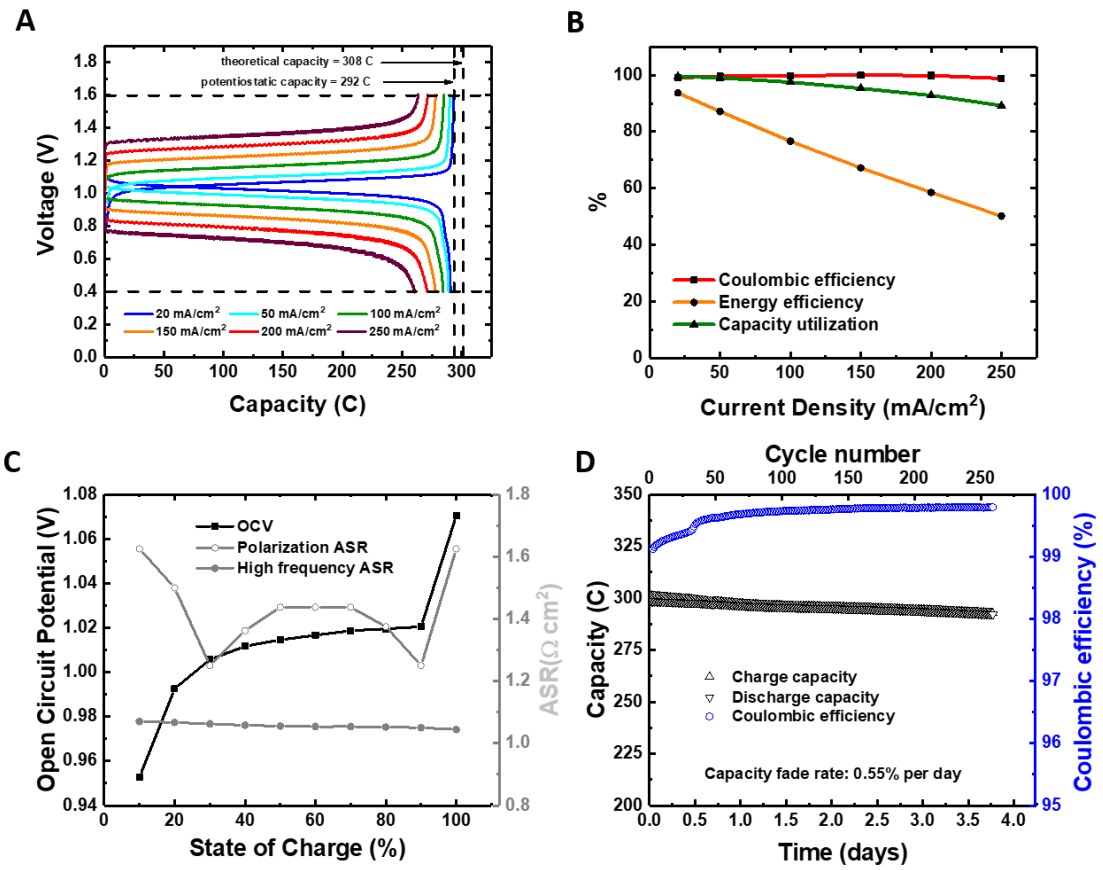

Figure 2. Full cell characterization of low concentration 0.1 M bislawsone. The negolyte comprised 8 mL of 0.1 M bislawsone in 1 M KOH while the non-limiting posolyte comprised 45 mL of 0.2 M potassium ferrocyanide and 0.02 M potassium ferricyanide in 1 M KOH solution. (A) Galvanostatic charge and discharge curves from 20 to 250 mA/cm^2. The vertical dashed lines indicate the maximum capacity realized with potentiostatic charge and discharge at the voltage cutoffs (1.6 and 0.4 V, respectively), as well as the theoretical capacity. (B) Coulombic efficiency, round-trip energy efficiency, and capacity utilization as a percentage of potentiostatic capacity versus current density. (C) OCV, high-frequency ASR, and polarization ASR versus SOC. (D) Coulombic efficiency (circle) and charge (upward-pointing triangles) and discharge (downward-pointing triangles) capacity versus time and cycle number for a negolyte-limited bislawsone cell. The cell was cycled galvanostatically at 100 mA/cm^2 for 3.8 days. The cell was cycled between 1.4 and 0.5 V, and each half cycle ended with a potentiostatic hold until the magnitude of the current density fell below 2 mA/cm^2.

To confirm that all four electrons in bislawsone can be accessed reversibly, the cell was cycled at different current densities ranging from 20 mA/cm^2 to 250 mA/cm^2 (**Figure 2A**). For each current density tested, a > 99% coulombic efficiency and > 90% capacity utilization were achieved based on the four-electron experimental potentiostatic capacity. A capacity utilization of 97.5% and round-trip energy efficiency of 77% was reached at 100 mA/cm^2

(**Figure 2B**). The nuclear magnetic resonance (NMR) spectrum of a charged negolyte showed a clean conversion to the fully reduced bislawsone (Figure S6). The high capacity utilization at high current density demonstrated that the dimerization strategy does not negatively affect the kinetics and accessed capacity.

A charging current of 100 mA/cm^2 was applied to charge the cell, and polarization curves were measured at 20, 50, and 100% states of quinone charge (SOC). The open circuit voltage (OCV) is 1.01 V at 50% SOC and 1.07 V at 100% SOC (**Figure 2C**), consistent with CV measurement. The membrane resistance contributed the largest fraction of the overall resistance; it can possibly be decreased in the future by manipulating the electrolyte composition and by decreasing the membrane thickness. The polarization curve (Figure S7) shows no sign of redox kinetic limitations and exhibits a peak galvanic power density exceeding 0.20 W cm^{-2}.

The viability of a flow battery hinges on the long-term stability of the system. Molecular stability has been a major concern for organic-based flow battery systems as there are many potential degradation pathways for organic molecules. Capacity fade may have both temporal or electrochemical cycling contributions, with the former dominating the lifetimes of the organic molecules that have been carefully studied to date.[27] To investigate the long-term stability of bislawsone, prolonged galvanostatic cycling of the 0.1 M bislawsone cell was performed at 100 mA/cm^2. In order to avoid temporal variations in accessed capacity and to ensure that 100% of the redox-active material was cycled, potential holds at 1.4 V and 0.5 V were applied until the magnitude of the current density fell below 2 mA/cm^2. 95% of theoretical capacity was accessed. The 5% discrepancy may be due to material transfer and residual water in the synthesized bislawsone powder. Over a 3.8-day period of cycling, a 2% capacity loss was observed, which corresponds to a capacity fade rate of 0.55% per day, or 0.008% per cycle. The cell maintained an average of 99.5% coulombic efficiency, and membrane resistance remained unchanged before and after the cycling. The capacity fade rate

indicates that the lifetime is approximately an order of magnitude longer than that of unprotected lawsone,[21-22] demonstrating the protective effect of the dimerization strategy employed

To investigate the performance at high concentration, a 0.5 M bislawsone cell (2 M electrons, 53.6 Ah/L) was constructed. All four electrons per molecule were accessed at high concentration, as shown in **Figure 3A**, leading to a 95.5% capacity utilization even at 300 mA cm^{-2} (**Figure 3B**). This near-quantitative capacity utilization at high current density has not been reported before to our knowledge in alkaline organic flow battery systems, which are usually limited by cell resistance and molecular diffusion. At 400 mA/cm^2, a lower capacity (80.0%) was accessed because membrane resistance dominated the voltage profile and the cell voltage quickly reached the 1.6 V and 0.4 V voltage cutoffs. At 100 mA/cm^2, 97.7% of the capacity was reversibly accessed with a Coulombic efficiency of 99.7% and round-trip energy efficiency of 79.3%, representing a significant improvement over a lawsone flow battery which had 70% accessed capacity and 68% round-trip energy efficiency.[25] The OCV of the 0.5 M bislawsone cell displayed typical Nernstian behavior with respect to SOC (Figure S8). A peak galvanic power density of 0.28 W/cm^2 was achieved as determined by the polarization curve at near 100% SOC (**Figure 3C**). The power density is mainly limited by high frequency area specific resistance. This is dominated by the membrane resistance (Figure S8), which is above 1 $\Omega \cdot cm^2$; it can possibly be decreased in the future by manipulating the electrolyte composition and by using a membrane with better conductivity.

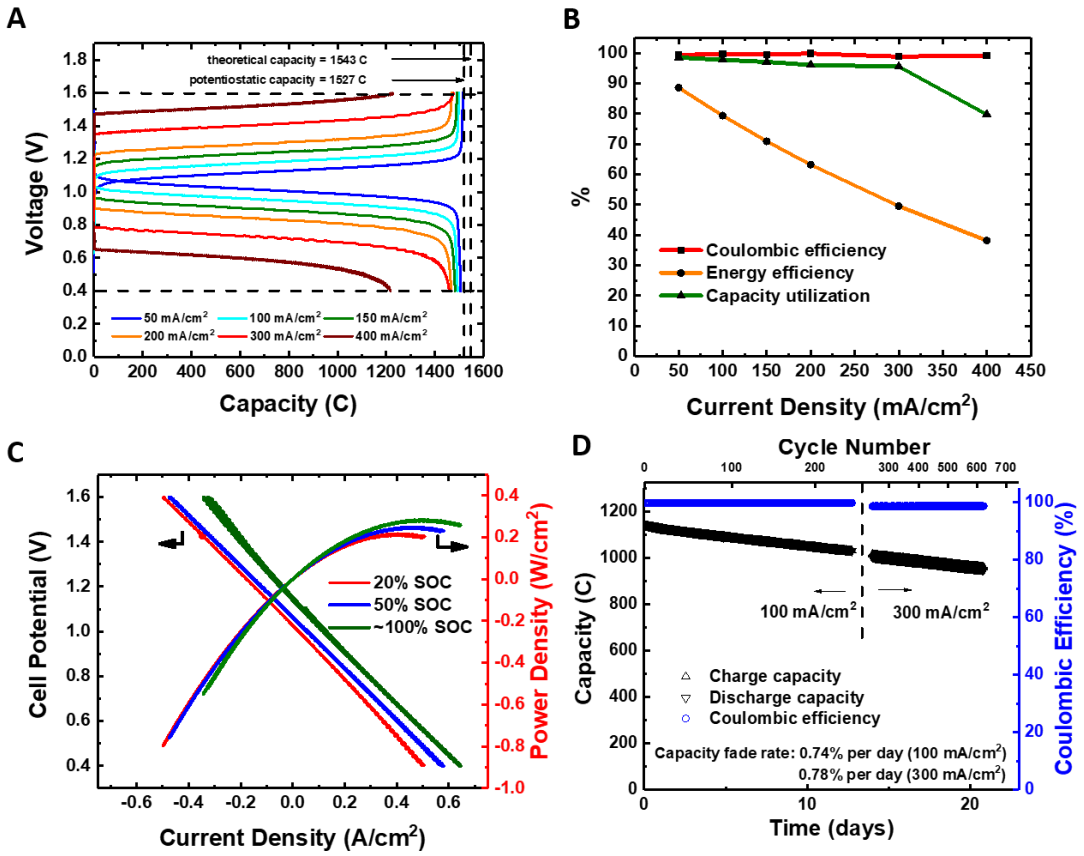

Figure 3. Full cell characterization of high concentration 0.5 M bislawsone. The negolyte comprised 8 mL of 0.5 M bislawsone in 1 M KOH while the non-limiting posolyte comprised 95 mL of 0.3 M potassium ferrocyanide and 0.1 M potassium ferricyanide in 1 M KOH solution. (A) Galvanostatic charge-discharge voltage profiles from 50 to 400 mA/cm^2. The vertical dashed lines indicate the maximum capacity realized with potentiostatic charge and discharge at the voltage cutoffs (1.6 and 0.4 V, respectively), as well as the theoretical capacity. (B) Coulombic efficiency, round-trip energy efficiency, and capacity utilization as a percentage of potentiostatic capacity versus current density. (C) Cell voltage versus discharge current density at room temperature at 10%, 30%, 50%, 70%, 90%, and 100% SOC. (D) Coulombic efficiency (circles), charge (upward-pointing triangles) and discharge (downward pointing triangles) capacity versus time and cycle number for a negolyte-limited bislawsone cell. The cell was cycled galvanostatically at 100 mA/cm^2 for 12.8 days and then rested for 1.2 days before switching to 300 mA/cm^2 for 6.8 days. The cell was cycled between 1.4 and 0.5 V, and each half cycle ended with a potentiostatic hold until the magnitude of the current density fell below 2 mA/cm^2. The volume of negolyte with same composition used was 6 mL in (D).

Long-term galvanostatic cycling of the 0.5 M bislawsone cell was performed at 100 mA cm^{-2} with potential holds at 1.4 V for charging and 0.5 V for discharging until the current density dropped to 2 mA/cm^2 (**Figure 3D**). 98.3% of the theoretical capacity was accessed. After 12.8 days of cycling, the capacity had faded by 9.5%, which corresponds to a temporal

capacity fade of 0.74% per day, or 0.038% per cycle. Because an excess amount of posolyte ferrocyanide and ferricyanide were used in the cycling, we attribute the slow capacity fade to the bislawsone negolyte. The per cycle capacity fade in the high concentration cell was superficially higher compared to low concentration cell due to longer per cycle cycling time in high concentration cell. The per day capacity fade rate is similar to that of low concentration cell (0.74% vs 0.55% per day), indicating that the stability of bislawsone is time dependent rather than cycle dependent.

Encouraged by our high capacity utilization at high current density, we cycled the 0.5 M bislawsone cell at a higher current density of 300 mA/cm^2. The cell maintained high capacity rate and stable charging/discharging plateau during the 6.8 days of continuous cycling with 98.8% coulombic efficiency. The cell lost 5.3% of its capacity, which corresponds to 0.78% loss per day. This rate is almost identical to the 0.74%/day loss rate when cycled at 100 mA/cm^2, demonstrating that bislawsone can be cycled at high current density under alkaline conditions without compromising its stability.

Investigation and potential mitigation of chemical degradation. Different strategies have been made in the field to synthesize more stable derivatives based on various redox-active scaffolds. However, the chemical space available for organic molecules is huge. Therefore, it is important to understand how a scaffold molecule degrades in order to rationally design the next generation of molecules with better performance. Despite the fact that bislawsone can inhibit Michael-addition decomposition pathway as compared to lawsone, capacity loss in our system was still observed. We have recently elucidated the molecular degradation mechanism of anthraquinones in flow batteries using 2,6-dihydroxyanthraquinone as a model system.[28] We therefore studied the degradation of naphthoquinones using bislawsone as a model system. A sample was taken from the above cycled discharged 0.5 M cell and subjected to NMR analysis. One major side product was observed which accounts for 14.2% of total NMR active

material (Figure S9). High-resolution liquid chromatography mass spectrometry (LC-MS) analysis found only one major side product with the mass to charge ratio of 347.0559 in negative ionization mode (Figure S10). Back calculation of the neutral mass gives $C_{20}H_{12}O_6$ as the molecular formula, which coincides in mass with a partial (2-electron) reduction of bislawsone starting material $C_{20}H_{10}O_6$.

In order to elucidate the chemical structure, the degradation product was isolated by preparative-scale high performance liquid chromatography (pHPLC, Figure S11). ^{1}H, 13C, and 2D NMR analysis on the purified degradation product showed the asymmetry between two monomer units, and the presence of two aliphatic proton peaks with doublet splitting patterns (Figure S12-S14) indicated a disruption in the conjugated system. Together, the NMR and LC-MS analyses are consistent with the structure where the bond between C2 and C3 of the bislawsone is reduced to a carbon-carbon single bond, locking the quinone unit into a di-ketone molecule, 2,3-dihydrobislawsone **4** (**Figure 4A**, type 1 tautomerization). Electrochemical reduction of a ketone into an alcohol and re-oxidation of the alcohol back to the ketone have high overpotentials and usually require a metal or organic catalyst[29-32]; therefore this side product should generally be considered as redox-inactive in a catalyst-free flow battery system using a carbon-based electrode. Because the similar degradation rate suggests a concentration and rate-independent degradation mechanism, the production of 2,3-dihydrobislawsone is not due to the direct reduction or oxidization by the electrode, but rather by the enol-ketone tautomerization of the partially reduced quinone-hydroquinone molecule, which is a process governed by kinetics and thermal equilibrium. The degradation of bislawsone into 2,3-dihydrobislawsone may be a general degradation mechanism for naphthoquinones. This conclusion is backed by some earlier studies, [33-34] which documented the tautomerization of reduced naphthoquinone. While this tautomerization was observed in many different naphthoquinone derivatives in earlier studies, the equilibrium and kinetics were heavily influenced by the substitution groups on the naphthoquinone ring. In this work,

the 2,3-dihydrobislawsone did not tautomerize back to the half-reduced hydroquinone form **2**, as the isolated 2,3-dihydrobislawsone was stable in air and alkaline solution. Given this general phenomenon, we expect that the tautomerization should also occur for the fully reduced bislawsone **3** at a different rate (Figure 4A, type 2), that can eventually result in a 4-electron reduction 2,2`,3,3`-tetrahydrobislawsone form **6** (tetra-ketone instead of bi-quinone) that is completely redox inactive). Indeed, careful LC-MS analysis of a discharged sample also found a molecule at a much lower concentration with an atomic mass that corresponds to a 4-electron reduction product after cycling (Figure S15). This molecule cannot be fully reduced bislawsone **3** because the sample was taken at the fully discharged state and exposed to air prior to analysis, and therefore is expected to be the redox-inactive tetra-ketone form.

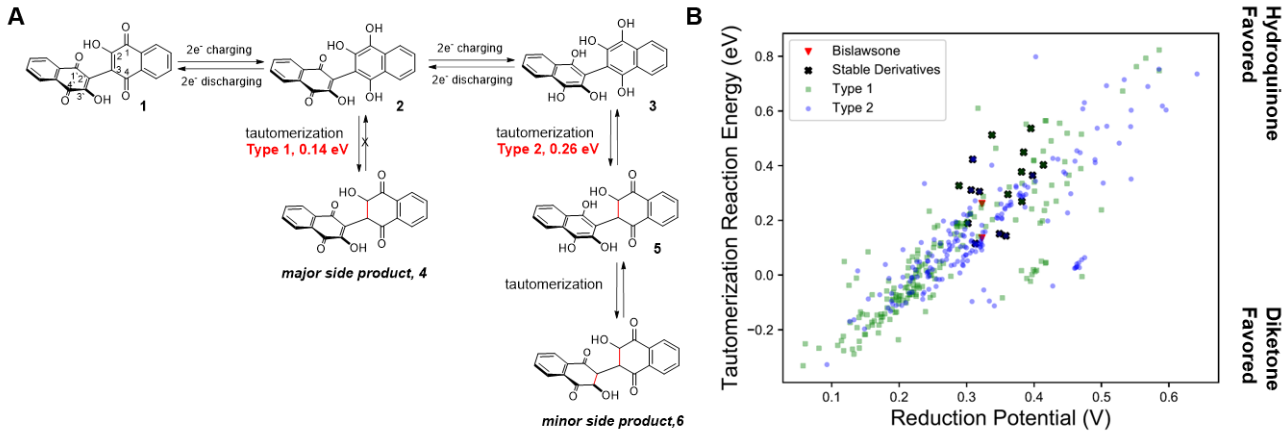

Figure 4. Decomposition study and theoretical calculations. (A) Scheme of decomposition pathway. The red text shows the calculated reaction energies of the reduced forms tautomerizing as calculated at the B3LYP/6-311+G(d,p) (PCM) level of theory. (B) Calculated tautomerization reaction energies plotted against calculated reduction potential of the couple. Type 1 and Type 2 refer to the nature of the intermediate: a "half-reduced" molecule (Type 1) or a fully reduced molecule (Type 2). Bislawsone is labeled with red triangle and 8 stable derivatives within 0.1 V of bislawsone reduction potential are labeled with black squares.

Based on the structure of degradation product, the degradation of bislawsone into the di-ketone form **4** should disrupt only half of the redox activity, as the other lawsone monomer unit stayed intact. Therefore, 2,3-dihydrobislawsone **4**, which accounts for 14.2% of total NMR active material, should only impact 7.1% of total capacity. However, 14.8% of the

capacity was lost in 21 days of cycling. There are several possibilities to account for the 7.7% difference. First, once reduced naphthoquinone **2** tautomerized into diketone form **4**, the 2-hydroxy group changed from a low-pKa phenol group into a high-pKa alcohol group, and would stay protonated in alkaline solution. Therefore, the solubility of 2,3-dihydrobislawsone molecule is expected to drop drastically and precipitate out of the solution, making it practically redox-inactive. Precipitate was indeed observed in electrolyte that has been cycled for a long-time. Second, the tetra-ketone form, 2,2`,3,3`-tetrahydrobislawsone **6**, accounts for 1% of the degradation product as detected by LC-MS, but its concentration is too low to be detected in NMR, and is expected to have even lower solubility due to the transformation of two solubilizing phenol groups into two alcohol groups. Other minor degradation products or NMR silent species and cell leakage may also contribute to the remaining capacity fade.

The equilibrium of hydroquinone-diketone is heavily influenced by the substituents on the naphthoquinone core; therefore, this presents an opportunity for a next generation naphthoquinone with a rationally designed substituent group. We have calculated (see the "Theoretical Calculation" section in Supporting Information) the stability and reduction potentials of 637 lawsone redox couples, which include 193 bislawsone derivatives. **Figure 4B** shows the correlation between the tautomer reaction energies and the predicted standard reduction potentials of redox couples. In general, lower reduction potentials are more likely to be subject to tautomerization than higher reduction potentials. Interestingly, despite the fact that the predicted standard reduction potentials of each of the two reductions of bislawsone are within 0.01 V of each other, the "type 1" decomposition is more thermodynamically favored than the "type 2" decomposition.

Of these, we predict that 8 bislawsone derivatives with reduction potentials within 0.1 V of bislawsone potentially have higher stability than bislawsone (Figure S16). One common motif in these stabilized molecules are oxy-alkyl substitutions, which have previously been shown to stabilize anthraquinone molecules against other decomposition mechanisms.[35] Our

calculations also indicate that the increased stability of bislawsone can be at least partially attributed to its protection against a tautomerization reaction relative to lawsone. Efforts to synthesize a more stable naphthoquinone are underway.

3. Conclusion

In summary, we demonstrate that dimerization is a promising synthetic strategy to improve the performance of quinone-based flow batteries. The bislawsone flow battery reported in this work delivered a high negolyte volumetric capacity, theoretically 53.6 Ah/L (2 M electrons), with peak power density of 0.28 W/cm^2. It reversibly accessed > 95.5% of theoretical capacity at a current density of 300 mA/cm^2 with significantly improved permeability and stability, making naphthoquinone a more practical redox-active negolyte in AORFBs. We identified tautomerization of the reduced naphthoquinone to the redox-inactive ketone form as a degradation mechanism of naphthoquinone in flow batteries. This mechanistic insight allowed us to propose more stable naphthoquinones and rationally design next generation organics for AORFB which could accelerate the use of wind and photovoltaic electricity.

Author Contributions

L.T. conceived the idea, developed the synthesis, and performed molecular characterization. E.M.F. and L.T. performed rotating disk electrode characterization. E.F.K. performed additional synthesis and measured solubility and viscosity. D.D.P performed permeability measurements. D.P.T. developed the molecular library and performed the theoretical stability calculations. Cell performance and electrolyte analysis were performed by L.T. and M.-A.G. The chemical degradation study was performed by L.T. The manuscript was drafted by L.T. and D.P.T. and revised by all authors. R.G.G. and M.J.A. supervised the experimental research and A.A.-G. supervised the theoretical research.

Acknowledgements

This work was supported in part by the following organizations: the U.S. Department of Energy Contract No. DE-AC05-76RL01830 through PNNL Subcontract No. 428977; Innovation Fund Denmark via the Grand Solutions project "ORBATS" file no. 7046-00018B; and the Massachusetts Clean Energy Technology Center. The authors thank Dr. David Kwabi and Shijian Jin for assistance and helpful discussions on experimental techniques.

References

1. Dunn, B.; Kamath, H.; Tarascon, J.-M., Electrical Energy Storage for the Grid: A Battery of Choices. *Science* **2011,** *334* (6058), 928.
2. Huskinson, B., Marshak, M. P., Suh, C., Er, S., Gerhardt, M. R., Galvin, C. J., Chen, X., Aspuru-Guzik, A., Gordon, R. G., Aziz, M. J., A metal-free organic-inorganic aqueous flow battery. *Nature* **2014,** *505* (7482), 195.
3. Yang, B., Hoober-Burkhardt, L., Wang, F., Surya Prakash, G. K., Narayanan, S. R., An inexpensive aqueous flow battery for large-scale electrical energy storage based on water-soluble organic redox couples. *J. Electrochem. Soc.* **2014,** *161*, A1371.
4. Lin, K.; Chen, Q.; Gerhardt, M. R.; Tong, L.; Kim, S. B.; Eisenach, L.; Valle, A. W.; Hardee, D.; Gordon, R. G.; Aziz, M. J.; Marshak, M. P., Alkaline quinone flow battery. *Science* **2015,** *349* (6255), 1529.
5. Yang, B.; Hoober-Burkhardt, L.; Krishnamoorthy, S.; Murali, A.; Prakash, G. K. S.; Narayanan, S. R., High-Performance Aqueous Organic Flow Battery with Quinone-Based Redox Couples at Both Electrodes. *J. Electrochem. Soc.* **2016,** *163* (7), A1442.
6. Yang, Z.; Tong, L.; Tabor, D. P.; Beh, E. S.; Goulet, M.-A.; De Porcellinis, D.; Aspuru-Guzik, A.; Gordon, R. G.; Aziz, M. J., Alkaline Benzoquinone Aqueous Flow Battery for Large-Scale Storage of Electrical Energy. *Adv. Energy Mater.* **2017**, 1702056.
7. Gerhardt, M. R.; Tong, L.; Gómez-Bombarelli, R.; Chen, Q.; Marshak, M. P.; Galvin, C. J.; Aspuru-Guzik, A.; Gordon, R. G.; Aziz, M. J., Anthraquinone Derivatives in Aqueous Flow Batteries. *Adv. Energy Mater.* **2017,** *7* (8), 1601488.
8. Cao, J.; Tao, M.; Chen, H.; Xu, J.; Chen, Z., A highly reversible anthraquinone-based anolyte for alkaline aqueous redox flow batteries. *J. Power Sources* **2018,** *386*, 40.
9. Kwabi, D. G.; Lin, K.; Ji, Y.; Kerr, E. F.; Goulet, M.-A.; De Porcellinis, D.; Tabor, D. P.; Pollack, D. A.; Aspuru-Guzik, A.; Gordon, R. G.; Aziz, M. J., Alkaline quinone flow battery with long lifetime at pH 12. *Joule* **2018,** *2*, 1907.
10. Liu, T.; Wei, X.; Nie, Z.; Sprenkle, V.; Wang, W., A Total Organic Aqueous Redox Flow Battery Employing a Low Cost and Sustainable Methyl Viologen Anolyte and 4-HO-TEMPO Catholyte. *Adv. Energy Mater.* **2015,** *6* (3), 1501449.
11. Janoschka, T.; Morgenstern, S.; Hiller, H.; Friebe, C.; Wolkersdorfer, K.; Hauptler, B.; Hager, M. D.; Schubert, U. S., Synthesis and characterization of TEMPO- and viologen-polymers for water-based redox-flow batteries. *Polym. Chem* **2015,** *6* (45), 7801.
12. DeBruler, C., Hu, B., Moss, J., Liu, X., Luo, J., Sun, Y., Liu, T. L., Designer two-electron storage viologen anolyte materials for neutral aqueous organic redox flow batteries. *Chem* **2017,** *3*, 1.
13. Janoschka, T.; Martin, N.; Hager, M. D.; Schubert, U. S., An aqueous redox-flow battery with high capacity and power: the TEMPTMA/MV system. *Angew. Chem. Int. Ed.* **2016,** *55* (46), 14427.
14. Beh, E. S., De Porcellinis, D., Gracia, R. L., Xia, K. T., Gordon, R. G., Aziz, M. J., A neutral pH aqueous organic–organometallic redox flow battery with extremely high capacity retention. *ACS Energy Lett.* **2017,** *2* (3), 639.
15. Hu, B.; DeBruler, C.; Rhodes, Z.; Liu, T. L., Long-cycling aqueous organic redox flow battery (AORFB) toward sustainable and safe energy storage. *J. Am. Chem. Soc.* **2017,** *139* (3), 1207.
16. Lin, K., Gómez-Bombarelli, R., Beh, E. S., Tong, L., Chen, Q., Valle, A., Aspuru-Guzik, A., Aziz, M. J., Gordon, R. G., A redox-flow battery with an alloxazine-based organic electrolyte. *Nat. Energy* **2016,** *1* (9), 16102.

17. Orita, A.; Verde, M. G.; Sakai, M.; Meng, Y. S., A biomimetic redox flow battery based on flavin mononucleotide. *Nat. Comm.* **2016,** *7*, 13230.
18. Hollas, A. W., X., Murugesan, V., Nie, Z., Li, B., Reed, D., Liu, J., Sprenkle, V., Wang, W., A biomimetic high-capacity phenazine-based anolyte for aqueous organic redox flow batteries. *Nat. Energy* **2018,** *3* (6), 508.
19. Winsberg, J.; Muench, S.; Hagemann, T.; Morgenstern, S.; Janoschka, T.; Billing, M.; Schacher, F. H.; Hauffman, G.; Gohy, J.-F.; Hoeppener, S.; Hager, M. D.; Schubert, U. S., Polymer/zinc hybrid-flow battery using block copolymer micelles featuring a TEMPO corona as catholyte. *Polym. Chem.* **2016,** *7* (9), 1711.
20. Dweck, A. C., Natural ingredients for colouring and styling. *Int. J. Cosmet. Sci.* **2002,** *24* (5), 287.
21. Wedege, K.; Drazevic, E.; Konya, D.; Bentien, A., Organic Redox Species in Aqueous Flow Batteries: Redox Potentials, Chemical Stability and Solubility. *Sci. Rep.* **2016,** *6*, 39101.
22. Hu, P.; Lan, H.; Wang, X.; Yang, Y.; Liu, X.; Wang, H.; Guo, L., Renewable-lawsone-based sustainable and high-voltage aqueous flow battery. *Energy Storage Mater.* **2018**.
23. Hoober-Burkhardt, L.; Krishnamoorthy, S.; Yang, B.; Murali, A.; Nirmalchandar, A.; Prakash, G. K. S.; Narayanan, S. R., A New Michael-Reaction-Resistant Benzoquinone for Aqueous Organic Redox Flow Batteries. *J. Electrochem. Soc.* **2017,** *164* (4), A600.
24. Tabor, D. P.; Gómez-Bombarelli, R.; Tong, L.; Gordon, R. G.; Aziz, M. J.; Aspuru-Guzik, A., Mapping the frontiers of quinone stability in aqueous media: implications for organic aqueous redox flow batteries. *J. Mater. Chem. A* **2019,** *7* (20), 12833.
25. Wang, C.; Yang, Z.; Wang, Y.; Zhao, P.; Yan, W.; Zhu, G.; Ma, L.; Yu, B.; Wang, L.; Li, G.; Liu, J.; Jin, Z., High-Performance Alkaline Organic Redox Flow Batteries Based on 2-Hydroxy-3-carboxy-1,4-naphthoquinone. *ACS Energy Lett.* **2018,** *3* (10), 2404.
26. Miller-Chou, B. A.; Koenig, J. L., A review of polymer dissolution. *Prog. Polym. Sci.* **2003,** *28* (8), 1223.
27. Goulet, M.-A.; Aziz, M. J., Flow Battery Molecular Reactant Stability Determined by Symmetric Cell Cycling Methods. *J. Electrochem. Soc.* **2018,** *165* (7), A1466.
28. Goulet, M.-A.; Tong, L.; Pollack, D. A.; Tabor, D. P.; Odom, S. A.; Aspuru-Guzik, A.; Kwan, E. E.; Gordon, R. G.; Aziz, M. J., Extending the Lifetime of Organic Flow Batteries via Redox State Management. *J. Am. Chem. Soc.* **2019,** *141* (20), 8014.
29. Badalyan, A.; Stahl, S. S., Cooperative electrocatalytic alcohol oxidation with electron-proton-transfer mediators. *Nature* **2016,** *535*, 406.
30. Weiss, C. J.; Wiedner, E. S.; Roberts, J. A. S.; Appel, A. M., Nickel phosphine catalysts with pendant amines for electrocatalytic oxidation of alcohols. *Chem. Comm.* **2015,** *51* (28), 6172.
31. Cheung, K.-C.; Wong, W.-L.; Ma, D.-L.; Lai, T.-S.; Wong, K.-Y., Transition metal complexes as electrocatalysts—Development and applications in electro-oxidation reactions. *Coord. Chem. Rev.* **2007,** *251* (17), 2367.
32. Francke, R.; Little, R. D., Redox catalysis in organic electrosynthesis: basic principles and recent developments. *Chem. Soc. Rev.* **2014,** *43* (8), 2492.
33. Bruce, D. B.; Thomson, R. H., 521. Aromatic keto-enols. Part II. Some new 2 : 3-dihydro-1 : 4-naphthaquinones and -anthraquinones. *J. Chem. Soc.* **1952**, 2759.
34. Thomson, R. H., 352. The structure of β-hydrojuglone and related compounds. Keto–;enols of the naphthalene series. *J. Chem. Soc.* **1950**, 1737.
35. Kwabi, D. G.; Lin, K.; Ji, Y.; Kerr, E. F.; Goulet, M.-A.; DePorcellinis, D.; Tabor, D. P.; Pollack, D. A.; Aspuru-Guzik, A.; Gordon, R. G.; Aziz, M. J., Alkaline quinone flow battery with long lifetime at pH 12. *Joule* **2018,** *2*, 1907.